

# High-efficiency solar cells on n-type HP mc-Si

Jan Benick, Florian Schindler, Stephan Riepe, Patricia Krenckel, Armin Richter, Ralph Müller, Hubert Hauser, Frank Feldmann, Bernhard Michl, Martin C. Schubert, Martin Hermle, Andreas Bett & Stefan W. Glunz, Fraunhofer ISE, Freiburg, Germany

Market Watch

Fab & Facilities

Materials

Cell Processing

Thin Film

PV Modules

## ABSTRACT

N-type high-performance multicrystalline silicon (HP mc-Si) has proved to have an excellent material quality. This paper presents details of the growth of HP mc-Si, as well as the properties of this material and its use in the fabrication of high-efficiency solar cells. The electrical material quality (charge-carrier lifetime) of mc-Si can be significantly improved by replacing the standard crystallization process with a seed-assisted growth for the crystallization of HP mc-Si. However, judging by the material quality for the application to high-efficiency solar cells, not only is the charge-carrier lifetime of crucial importance for the efficiency potential, but also other material properties, such as the base resistivity, are significant. Applying the optimal mc material, an analysis based on device simulation reveals an efficiency potential of the order of 22.4%. Finally, the results are shown for n-type HP mc-Si solar cells with a diffused boron front emitter and a full-area passivating rear contact (TOPCon). A certified efficiency of 21.9% is demonstrated, which represents the highest efficiency reported so far for multicrystalline silicon solar cells.

## Introduction

Increasing solar cell efficiency is a powerful lever for further cost reductions in photovoltaics. For industrial-type screen-printed p-type solar cells on monocrystalline silicon, efficiencies of up to 22.6% have so far been reported [1], whereas for a comparably processed p-type solar cell on multicrystalline silicon (mc-Si), the highest certified efficiencies reported to date are 21.3% [2] and 21.6% [3]. Even so, p-type mc-Si accounts for ~70% of global solar cell production [4]. Although mc-Si suffers from a higher carrier recombination caused by structural defects and a higher concentration of impurities, the simpler crystallization process used offers a cost advantage potential over monocrystalline silicon.

The highest efficiencies for silicon solar cells so far, however, have been achieved with n-type silicon, with a record efficiency of 26.7% being reported for an interdigitated back-contact (IBC) solar cell [5]. The high material quality of n-type silicon is mainly due to its relative tolerance to common impurities (e.g. Fe), resulting in higher minority-carrier diffusion lengths compared with p-type substrates with a similar impurity concentration [6]. With advances in crystallization techniques, such as seed-assisted growth for the fabrication of high-performance multicrystalline silicon (HP mc-Si) [7], the material quality of mc-Si wafers has significantly increased in recent years, mainly because of a reduced density

of recombination-active dislocation clusters.

The HP mc-Si process, combined with the above-mentioned benefits of n-type silicon, might therefore offer opportunities for a low-cost, high-efficiency silicon material which has the potential to reduce the efficiency gap with monocrystalline silicon [8]. This paper describes the fabrication process for a high-efficiency solar cell with a passivating rear-side contact (TOPCon [9]) on high-quality n-type HP mc-Si.

“The development of HP mc-Si has made it possible to significantly improve the material quality of mc-Si.”

## Material development

The crystallization of n-type mc-Si at Fraunhofer ISE started several years ago with the crystallization of standard n-type mc-Si. A comparison of that material with p-type mc-Si from a comparable crystallization process revealed an advantage of n-type doped mc-Si as a result of its lower sensitivity to typical metal impurities [10]. The development of HP mc-Si [7] has made it possible to significantly improve the material quality of mc-Si. With the use of granular silicon as seed material placed on the bottom of the crucible, a homogeneous and small-grained crystal structure was developed for the laboratory ingots of G2 size, equivalent to 75kg of silicon (Fig. 1). This led to a massive reduction in dislocation density and thus to an improvement in minority-carrier lifetime in the wafers.

In 2015 n-type HP mc-Si crystallized

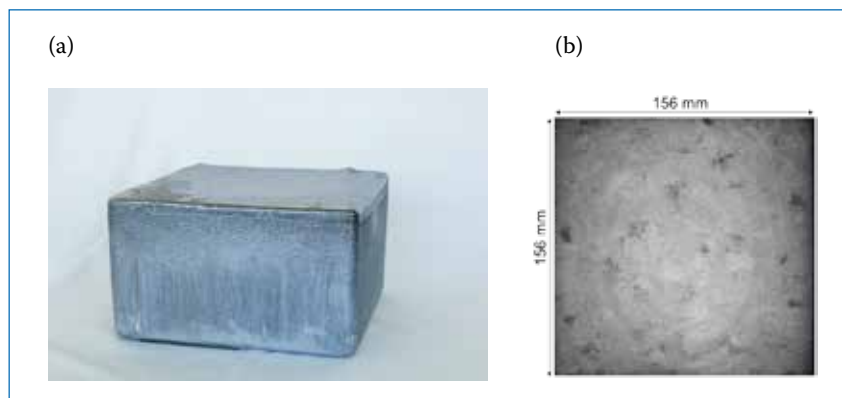


Figure 1. (a) An n-type HP mc-Si ingot of G2 size. (b) Photoluminescence image of a wafer from a centre brick in the upper third of an HP mc-Si ingot.

at Fraunhofer ISE was demonstrated to be a suitable base material for high-efficiency solar cells, with the achievement of an efficiency of 19.6% from an n-type mc-Si solar cell featuring a passivating rear-side contact (TOPCon [9]) and an isotextured front surface [8]. The crystallization process for HP mc-Si was recently further optimized by the use of high-purity crucibles and improved thermal processes, and the base resistivity was adapted in order to be optimally suited to the TOPCon cell concept.

### Analysis of material potential

To demonstrate the improvement in the material quality of n-type mc-Si crystallized at Fraunhofer ISE, a thorough efficiency analysis of three materials was performed: 1) standard n-type mc-Si; 2) n-type HP mc-Si; and 3) optimized n-type HP mc-Si. For the investigation of the material quality, lifetime samples were processed by applying the high-temperature steps of the utilized solar cell process sequence, including a boron diffusion at 890°C and an annealing step at 800°C (both for 1h). Thus, it was ensured that the material quality of the lifetime samples corresponded to the material quality of the final solar cells.

To ensure an injection-independent surface passivation, the samples were passivated with SiN<sub>x</sub> films.

Images of the bulk minority-charge carrier lifetime were obtained by injection-dependent photoluminescence (PL) imaging, calibrated by modulated PL [11]. A combination of these images with a PC1D [12,13] simulation of the TOPCon cell enables a prediction of the material's efficiency potential by an efficiency-limiting bulk recombination analysis (ELBA) [14], as well as allowing a detailed loss analysis, as suggested in Schindler et al. [15]. Further information about the procedure and the simulation parameters, as well as details about an investigation of the impact of the base resistivity, can be found in Schindler et al. [16].

Fig. 2(a) shows predictions of the spatially resolved efficiency potential of the three materials. The corresponding material-related efficiency losses with regard to the simulated device limit (no Shockley-Read-Hall (SRH) material limitations) of 23.1% are illustrated in Fig. 2(b). The largest losses of ~2.4%<sub>abs.</sub> occur in the n-type mc-Si created from a standard crystallization process: these losses can be separated into inner grain losses (~1%<sub>abs.</sub>, orange part of the left

bar in Fig. 2(b)), and losses due to recombination-active structural crystal defects (~1.4%<sub>abs.</sub>, grey meshed part of the left bar in Fig. 2(b)). Consequently, the efficiency of a TOPCon solar cell based on this material would be limited to approximately 20.7%.

The HP mc-Si crystallization process suppresses the creation of highly recombination-active dislocation clusters, while the use of a high-purity crucible reduces the inner grain losses due to homogeneously distributed impurities. A significant reduction in efficiency losses is therefore observed for the second material: the n-type HP mc-Si features inner grain losses of ~0.3%<sub>abs.</sub> and losses of ~0.7%<sub>abs.</sub> due to recombination-active structural crystal defects, which sum up to total efficiency losses of ~1%<sub>abs.</sub> (see centre column in Fig. 2).

Finally, by optimizing the HP mc-Si crystallization process it is possible to decrease the area fraction of grain boundaries and consequently reduce the losses due to recombination-active structural crystal defects. In combination with an adaptation of the base resistivity, the total losses could be reduced to ~0.7%<sub>abs.</sub> for the optimized n-type HP mc-Si, which would allow efficiencies of the order of 22.4% (see right column in Fig. 2) with the TOPCon cell concept.

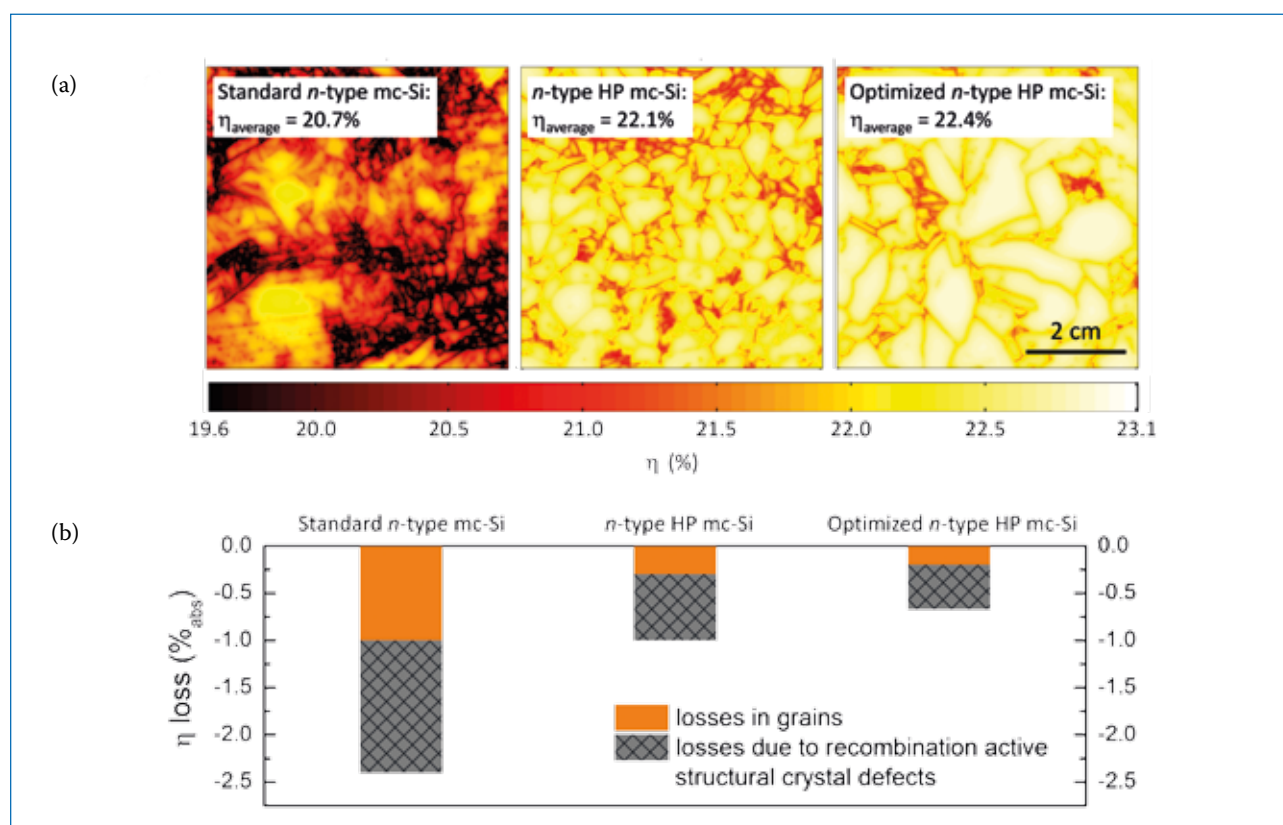


Figure 2. (a) ELBA prediction of the spatially resolved efficiency potential for the three different n-type mc-Si materials – standard, high-performance and optimized high-performance crystallization process; (b) corresponding solar cell efficiency losses.

It should be noted that the gain in efficiency potential for the optimized n-type HP mc-Si material was partly achieved by the correct choice of base resistivity. Fig. 3 shows a simulation of the efficiency as a function of base resistivity for two different materials, for the TOPCon cell concept described above. A defect-free material is limited by Auger recombination at low resistivities, and features an increasing efficiency with increasing base resistivity (orange dashed curve in the lower graph of Fig. 3). In contrast, a material with an injection-independent background lifetime of 1ms is also limited by Auger recombination for very low resistivities, but the efficiency reaches a maximum at a base resistivity of  $\sim 0.45\Omega\text{-cm}$ , before it decreases again for higher resistivities.

The decrease at high resistivities is attributed to fill factor losses, as illustrated by the black solid line in the upper graph of Fig. 3, which shows the normalized cell parameters for the defect-limited material as a function of resistivity. The fill factor losses towards high resistivities are not a series-resistance effect, but rather a recombination effect which influences  $V_{mpp}$  and also leads to losses in the pseudo fill factor. The decrease towards lower resistivities is attributed to  $J_{sc}$  limitations caused by Auger recombination (black dotted line in the upper graph of Fig. 3). For n-type HP mc-Si, the correct choice of base resistivity is therefore of the utmost importance for fabricating highly efficient solar cells.

**“For n-type HP mc-Si, the correct choice of base resistivity is of the utmost importance for fabricating highly efficient solar cells.”**

### Surface texture

To suppress surface reflection of incident light, and thus maximize the current of a solar cell, specific structures have to be applied to the solar cell front side. These structures typically consist of a surface texture in combination with an anti-reflection coating. For monocrystalline silicon, the surface texture consists of small pyramids, which can be realized by anisotropic etching in alkaline solutions. When this texturing is used in combination with an anti-reflection coating, the weighted reflectance of such a surface can be as low as 2%.

In the case of mc-Si, however, the application of a pyramidal surface texture is not possible, because of the varying crystal orientations of the different grains; thus acidic solutions are used for the surface texturing of mc-Si solar cells in industrial production. Unfortunately, the quality of this type of surface texture does not match the excellent optical and electrical quality of pyramidal textures. Alternative technologies exist, however, which enable the creation of textures with a performance comparable to that of a pyramidal texture on mc-Si; two examples are the honeycomb texture [17,18] and black silicon [19,20].

The honeycomb texture (based on photolithography) has already been applied to the multicrystalline record solar cell (20.4% efficiency) presented by Schultz et al. in 2004 [17]. The other approach, which was also used for creating the surface texture of the high-efficiency HP mc-Si solar cells in this work, is based on black silicon; the nanostructured black-silicon surface enables an almost perfect suppression of the surface reflection, with values of less than 1% for the weighted reflectance. In the past, the surface passivation of this nanostructured surface with very steep needles (‘silicon grass’) was an issue, but this could fortunately be resolved by the introduction of deposited  $\text{Al}_2\text{O}_3$  layers (atomic layer deposition: ALD), which yield a very conformal coating even on black-silicon-textured surfaces [21–24].



**ILS-TT nx**  
Next Generation Turntable Platform

### HIGH THROUGHPUT LASER MACHINE

- Up to 6000 wafers per hour (w/h)
- Multi process head configuration
- Dual lane automation system
- Laser Contact Opening for PERC
- Laser Doped Selective Emitter
- Front side LCO
- Laser Direct Cleaving



VISIT US  
EU PV SEC  
B 9



InnoLas Solutions GmbH  
[www.innolas-solutions.com](http://www.innolas-solutions.com)

For the creation of black-silicon textures, typically reactive ion-etched (RIE) processes are utilized. In this study, however, an inductively coupled plasma (ICP) process with a very low bias voltage (as proposed in Hirsch et al. [25]) was employed in order to keep the surface damage due to the plasma etching as low as possible. With the ICP process, a separate damage etch prior to surface passivation is not necessary. An SEM micrograph of the surface texture realized by the ICP process is shown in Fig. 4: it can be seen that the texture does not feature the very steep needles typical of a classic black-silicon texture. The height of the texture is less than  $1\mu\text{m}$ , and the aspect ratio is around 2.

The corresponding reflectance measurements for assessing the optical quality of this surface texture are shown in Fig. 5. With just the surface texture, i.e. without the anti-reflection coating, the surface reflection is already quite low. When the measured reflectance is weighted with the sun spectrum (AM1.5g, 280–1,000nm), the total reflectance is of the order of 2.5%.

To further reduce the surface reflection, an anti-reflection coating can be added. In the current study a layer stack consisting of  $\text{Al}_2\text{O}_3$  (ALD) and  $\text{SiN}_x$  (plasma-enhanced chemical vapour deposition: PECVD) was applied. As can be seen in Fig. 5, the application of this anti-reflection coating further reduces the surface reflection, and values of  $\sim 1\%$  for the weighted reflectance can be achieved. The optical performance of the applied plasma texture is therefore comparable to that of a classic black-silicon texture.

In addition to an excellent optical performance, the front-side texture needs to demonstrate a high electrical quality (low surface recombination) as well as being compatible with subsequent processing steps, such as emitter diffusion and surface passivation. The results of the tests of

emitter diffusion ( $90\Omega/\text{sq.}$ ,  $\text{BBr}_3$  tube diffusion) and surface passivation by  $\text{Al}_2\text{O}_3$  (ALD) showed that the performance of the ICP black-silicon texture compared quite well with that of a pyramidal texture as applied to monocrystalline silicon, with values for the recombination pre-factor  $J_{0e}$  of the order of  $50\text{fA}/\text{cm}^2$ .

### Solar cells

On the basis of the excellent results obtained in respect of the material quality of n-type HP mc-Si, as well as the facility to implement all necessary process steps, high-efficiency solar cells were fabricated from the multicrystalline n-type silicon. The schematic of the solar cell is shown in Fig. 6: the features of the applied cell design (as discussed above)

are an ICP black-silicon surface texture, a  $\text{BBr}_3$ -diffused front-side emitter ( $90\Omega/\text{sq.}$ ) passivated by an  $\text{Al}_2\text{O}_3/\text{SiN}_x$  (ALD/PECVD) layer stack, and photolithographically defined and evaporated front contacts. The solar cell rear side incorporates a passivating contact consisting of a wet-chemically grown thin tunnel oxide covered by a PECVD-deposited a- $\text{SiC}_x\text{:P}$  layer (TOPCon [9]) with a full-area Ag metallization.

A photograph of a final high-efficiency solar cell fabricated on n-type HP mc-Si is shown in Fig. 7. Within the active cell area with the black-silicon texture, the grain structure of the multicrystalline silicon can no longer be seen – the cell area appears perfectly black. In the spaces between the active solar cells, however, the small grains of the HP mc-Si are clearly visible.

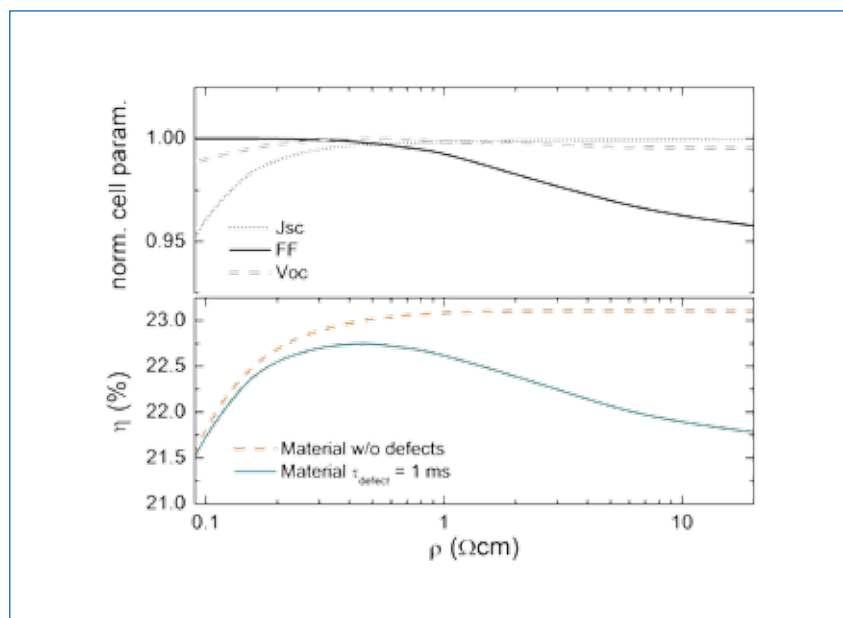


Figure 3. Impact of base resistivity on solar cell performance. The lower graph shows the conversion efficiency for a solar cell with a perfect material quality, as well as for a cell with a limited lifetime (injection-independent background lifetime of 1ms). The upper graph shows the normalized  $I-V$  parameters of the cell with the limited lifetime.

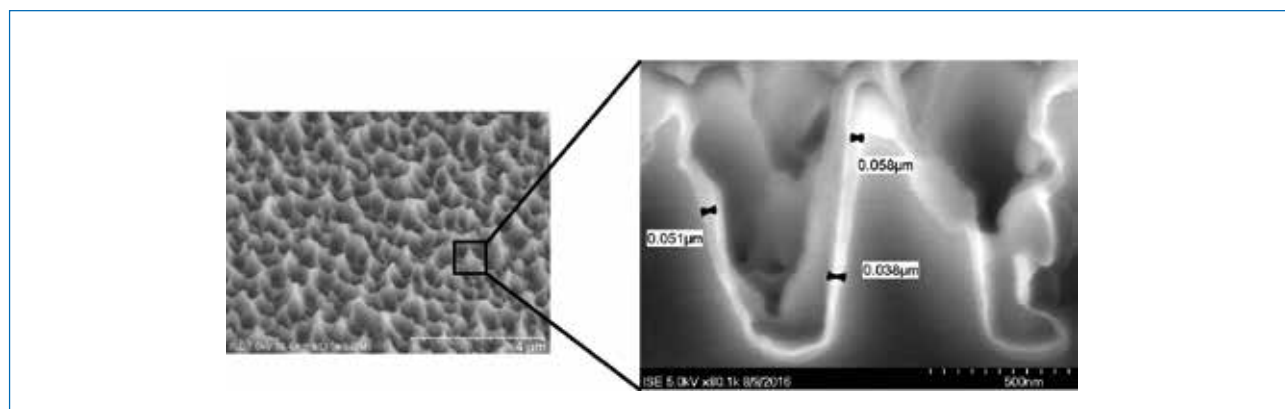


Figure 4. SEM micrograph of the front-side plasma texture (black silicon) on the n-type HP mc-Si. The micrograph on the right shows an enlargement of the surface texture with the  $\text{Al}_2\text{O}_3/\text{SiN}_x$  anti-reflection coating.

A summary of the corresponding  $I-V$  parameters measured for the best solar cells is shown in Table 1. In addition to the n-type HP mc-Si solar cells with a black-silicon texture, the table also includes the results for cells of the same material with a planar surface, as well as for reference solar cells made of n-type float-zone (FZ) silicon. It can be seen that the FZ reference solar cells delivered a high conversion efficiency of 23.3%, which is close to the maximum achievable using the applied technology (23.6%, based on device simulation [26]). This indicates that almost the full potential of the applied cell structure was exploited.

“The resulting conversion efficiency of the black-silicon-textured cells was 21.9%, which is the current world-record efficiency for a multicrystalline silicon solar cell.”

In the case of the multicrystalline solar cells with the black-silicon texture, a high open-circuit voltage  $V_{oc}$  of 672.6mV, a high short-circuit current density  $J_{sc}$  of 40.8mA/cm<sup>2</sup>, and a fill factor  $FF$  of 79.7% were obtained. The resulting conversion efficiency of the black-silicon-textured cells was 21.9%, which is the current world-record efficiency for a multicrystalline silicon solar cell.

A comparison of the multicrystalline solar cells with the black-silicon texture and with the planar front side reveals a small difference in  $V_{oc}$  of 3.5mV (676.1mV was measured for the planar solar cells). This difference represents an additional  $J_{0e}$  resulting from the surface texture of 20fA/cm<sup>2</sup>, which is exactly what would have been expected on the basis of lifetime test samples, and confirms that the passivation of the black-silicon texture by the  $Al_2O_3/SiN_x$  layer stack was effective. The comparable  $FF$  values for the planar and textured solar cells show that the surface texture did not have any detrimental effect on the front-side metallization. However, as can be seen from the FZ reference, the applied structure allows higher values for  $FF$  and  $pFF$ . As the  $pFF$  does not rely on series-resistance effects, and because the parallel resistance is sufficiently high (>4k $\Omega$ -cm<sup>2</sup>), the relatively low  $FF$  is most likely directly related either to the quality of the base material (e.g. recombination at the maximum power point (mpp)), or to effects connected with the

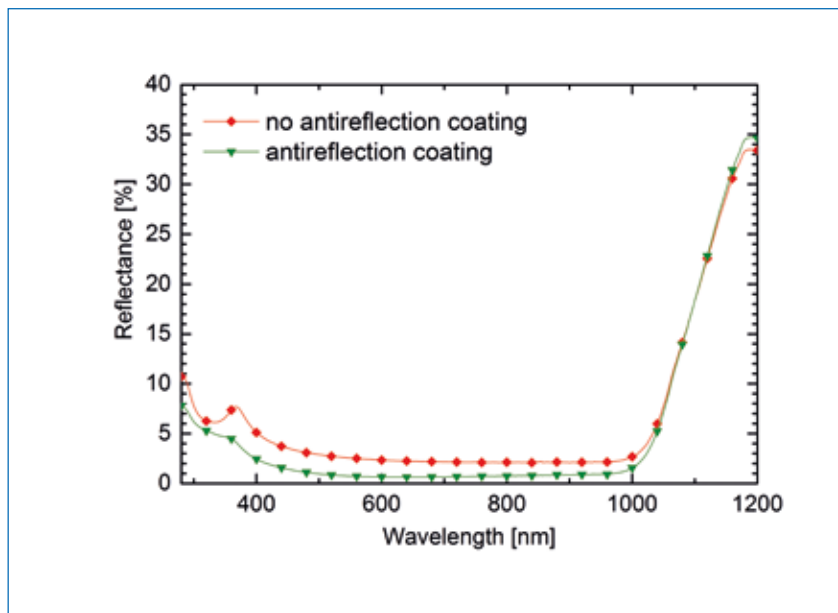


Figure 5. Measured reflectance of the black-silicon-like plasma texture without and with an  $Al_2O_3/SiN_x$  anti-reflection coating.

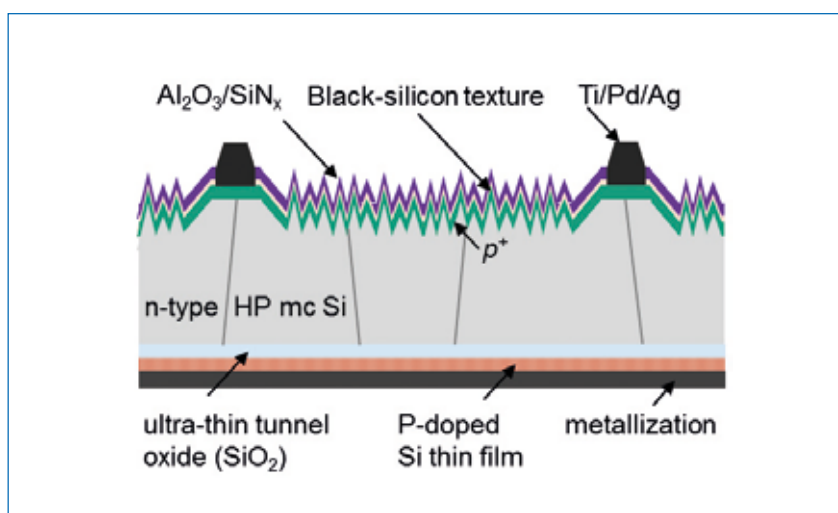


Figure 6. Schematic of the n-type HP mc-Si solar cell on multicrystalline silicon.

multicrystalline nature of the material.

The high  $J_{sc}$  (40.8mA/cm<sup>2</sup>) for the black-silicon texture indicates an effective reduction in the surface reflection. This reduction can be also seen in the reflectance curves shown in Fig. 8: the measured surface reflectance of the black-silicon cells (especially in the short-wavelength range) is even lower than the reflectance of the FZ reference solar cells with a pyramidal surface texture. As can be seen by the reflection in the long wavelength range, similar light trapping can be observed for both front-side structures. Nevertheless, the  $J_{sc}$  measured for the multicrystalline solar cells is less than the value for the FZ reference solar cells; this can be attributed to losses in the long wavelength range (see IQE curve in Fig. 8). As both cells feature the same rear-side structure (passivating contacts,

TOPCon), this difference is also most likely related to the base material.

## Conclusion and outlook

In the study reported in this paper it was demonstrated that n-type HP mc-Si is well suited to the fabrication of high-efficiency solar cells. The transition from standard mc-Si to an improved crystal structure with a low impurity concentration could reduce the material-related efficiency losses to about 0.5%<sub>abs</sub>, when the ideal base resistivity is utilized. On the assumption of a high-efficiency cell structure with passivating contacts (e.g. TOPCon), an efficiency potential well above 22% for the multicrystalline silicon is possible. When an adapted TOPCon cell fabrication process with a black-silicon front-surface texture and a 90 $\Omega$ /sq.  $Al_2O_3$ -passivated boron emitter

	$V_{oc}$ [mV]	$J_{sc}$ [mA/cm <sup>2</sup> ]	FF [%]	$pFF$ [%]	$\eta$ [%]
N-type FZ Si, random pyramids	683.9	41.5	82.2	84.1	23.3
N-type HP mc Si, planar surface	676.1	37.3	79.5	81.7	20.1
N-type HP mc Si, black-silicon texture	672.6	40.8	79.7	81.6	21.9*

\*Certified measurement by Fraunhofer ISE CalLab (4cm<sup>2</sup> aperture area).

**Table 1. Measured  $I-V$  parameters (AM1.5g, 100mW/cm<sup>2</sup>, 25°C) of the best FZ and HP mc-Si solar cells of each group (FZ – random pyramidal texture; HP mc-Si – planar surface or black-silicon-textured surface).**

was employed, a record efficiency of 21.9% was achieved for the n-type HP mc-Si solar cells.

“The implementation of an optimized technology is expected to bridge a significant portion of the efficiency gap with monocrystalline silicon.”

In future work the limitations of the multicrystalline silicon in combination with the processing steps needed for cell fabrication will be investigated in more detail in order to derive optimization strategies. The implementation of an optimized technology is expected to bridge a significant portion of the efficiency gap with monocrystalline silicon, thus raising the cost advantage potential of multicrystalline silicon.

**Acknowledgements**

The authors would like to thank F. Haas, P. Häuber, A. Leimenstoll, F. Schätzle, S. Seitz, A. Seiler, C. Harmel, R. van der Vossen and E. Schäffer for their support with the cell processing and measurements. The authors also would like to acknowledge Wacker Polysilicon for the silicon materials and fruitful discussions. This project was funded by the German Federal Ministry for Economic Affairs and Energy under Contract No. 0324034 (multiTOP).

**References**

[1] Trina Solar 2016, “Trina Solar announces new efficiency record of 22.61% for mono-crystalline silicon PERC cell”, Press release [http://phx.corporate-ir.net/phoenix.zhtml?c=206405&p=irol-newsArticle&ID=2230468].

[2] Deng, W. et al. 2016, “Development of high-efficiency industrial p-type multi-crystalline PERC solar cells with efficiency greater than 21%”, *Energy Procedia*, Vol. 92, pp. 721–729.

[3] Zheng, P. et al. 2017, “21.63% industrial screen-printed

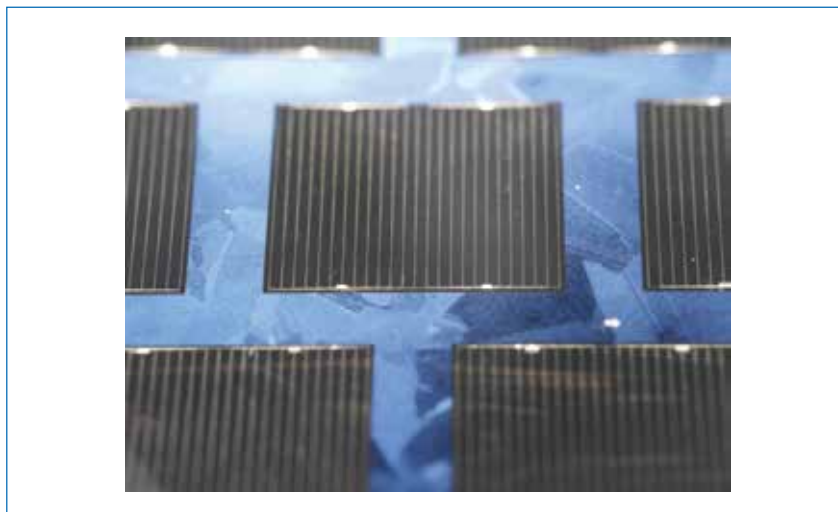


**Figure 7. Photograph of the final high-efficiency n-type HP mc-Si solar cell.**

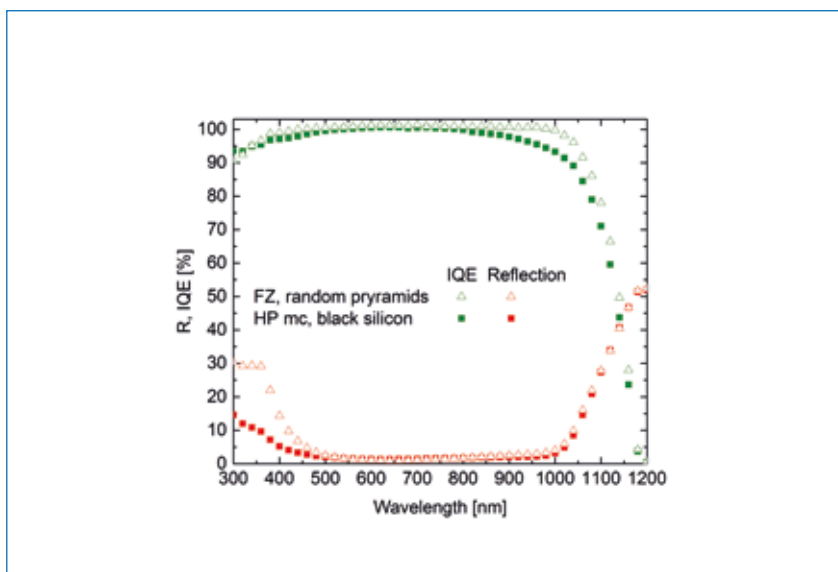


**Figure 8. Measured internal quantum efficiency (IQE) and reflection curves for the n-type HP mc-Si solar cell featuring a black-silicon surface texture, and for the n-type FZ reference solar cell with a random pyramidal texture.**

multicrystalline Si solar cell”, *physica status solidi (RRL)*, Vol. 11, No. 3.

[4] Fraunhofer ISE, “Renewable energy data”, Report [https://www.ise.fraunhofer.de/de/daten-zu-erneuerbaren-energien.html].

[5] Yoshikawa, K. et al. 2017, “Silicon heterojunction solar cell with interdigitated back contacts for a photoconversion efficiency over

26%”, *Nat. Energy*, Vol. 2, p. 17032.

[6] Macdonald, D. & Geerligs, L.J. 2004, “Recombination activity of interstitial iron and other transition metal point defects in p- and n-type crystalline silicon”, *Appl. Phys. Lett.*, Vol. 85, No. 18, pp. 4061–4063.

[7] Yang, Y.M. et al. 2015, “Development of high-performance multicrystalline

- silicon for photovoltaic industry”, *Prog. Photovolt: Res. Appl.*, Vol. 23, No. 3, pp. 340–351.
- [8] Schindler, F. et al. 2015, “High-efficiency multicrystalline silicon solar cells: Potential of n-type doping”, *IEEE J. Photovolt.*, Vol. 5, No. 6, pp. 1571–1579.
- [9] Feldmann, F. et al. 2014, “Passivated rear contacts for high-efficiency n-type Si solar cells providing high interface passivation quality and excellent transport characteristics”, *Sol. Energy Mater. Sol. Cells*, Vol. 120, pp. 270–274.
- [10] Schindler, F. et al. 2015, “Potential gain in multicrystalline silicon solar cell efficiency by n-type doping”, *IEEE J. Photovolt.*, Vol. 5, No. 2, pp. 499–506.
- [11] Giesecke, J.A. et al. 2011, “Minority carrier lifetime imaging of silicon wafers calibrated by quasi-steady-state photoluminescence”, *Sol. Energy Mater. Sol. Cells*, Vol. 95, No. 3, pp. 1011–1018.
- [12] Clugston, D.A. & Basore, P.A. 1997, “PC1D version 5: 32-bit solar cell modeling on personal computers”, *Proc. 26th IEEE PVSC*, Anaheim, California, USA, pp. 207–210.
- [13] Haug, H. et al. 2015, “PC1Dmod 6.1 – state-of-the-art models in a well-known interface for improved simulation of Si solar cells”, *Sol. Energy Mater. Sol. Cells*, Vol. 142, pp. 47–53.
- [14] Michl, B. et al. 2012, “Efficiency limiting bulk recombination in multicrystalline silicon solar cells”, *Sol. Energy Mater. Sol. Cells*, Vol. 98, pp. 441–447.
- [15] Schindler, F. et al. 2014, “Solar cell efficiency losses due to impurities from the crucible in multicrystalline silicon”, *IEEE J. Photovolt.*, Vol. 4, No. 1, pp. 122–129.
- [16] Schindler, F. et al. 2017, “Optimized multicrystalline silicon for solar cells enabling conversion efficiencies of 22%”, *Sol. Energy Mater. Sol. Cells*, Vol. 171, pp. 180–186.
- [17] Schultz, O. et al. 2004, “Multicrystalline silicon solar cells exceeding 20% efficiency”, *Prog. Photovolt: Res. Appl.*, Vol. 12, No. 7, pp. 553–558.
- [18] Hauser, H. et al. 2012, “Honeycomb texturing of silicon via nanoimprint lithography for solar cell applications”, *IEEE J. Photovolt.*, Vol. 2, No. 2, pp. 114–122.
- [19] Oh, J. et al. 2012, “An 18.2%-efficient black-silicon solar cell achieved through control of carrier recombination in nanostructures”, *Nature Nanotech.*, Vol. 7, No. 11, pp. 743–748.
- [20] Repo, P. et al. 2013, “N-type black silicon solar cells”, *Energy Procedia*, Vol. 38, pp. 866–871.
- [21] Algasinger, M. et al. 2013, “Improved black silicon for photovoltaic applications”, *Adv. Energy Mater.*, Vol. 3, No. 8, pp. 1068–1074.
- [22] Repo, P. et al. 2013, “Effective passivation of black silicon surfaces by atomic layer deposition”, *IEEE J. Photovolt.*, Vol. 3, No. 1, pp. 90–94.
- [23] Repo, P. et al. 2013, “Passivation of black silicon boron emitters with atomic layer deposited aluminum oxide”, *physica status solidi (RRL)*, Vol. 7, No. 11, pp. 950–954.
- [24] Otto, M. et al. 2012, “Extremely low surface recombination velocities in black silicon passivated by atomic layer deposition”, *Appl. Phys. Lett.*, Vol. 100, No. 19, p. 191603.
- [25] Hirsch, J. et al. 2016, “Optoelectronic properties of black-silicon generated through inductively coupled plasma (ICP) processing for crystalline silicon

# SOLAR & STORAGE FINANCE USA

30-31 OCTOBER 2017  
NEW YORK, USA

The only event that covers finance and investment for solar and storage in the U.S.

- Updates on tax equity deal-flow, M&A strategies, Community solar financing
- Energy Storage revenue stacking model, finance & investment and regional strategies
- Utilities role in solar M&A, storage deployment and procurement
- What are RTO/ISOs priorities
- Regional solar deployment round-tables

[financeusa.solarenergyevents.com](http://financeusa.solarenergyevents.com)

[marketing@solarmedia.co.uk](mailto:marketing@solarmedia.co.uk)

## Key Speakers Include:



GAF

Jason Barrett, Executive Director- Head of Renewable Energy Finance and Investment



BLACKROCK

David Giordano, Managing Director



STATE STREET BANK

Santosh Raikar, Managing Director



ALTUS POWER

Tom Athan, CEO

solar cells”, *Appl. Surface Sci.*, Vol. 374, pp. 252–256.

[26] Fell, A. 2013, “A free and fast three-dimensional/two-dimensional solar cell simulator featuring conductive boundary and quasi-neutrality approximations”, *IEEE Trans. Electron Dev.*, Vol. 60, No. 2, pp. 733–738.

#### About the Authors



**Jan Benick** studied microsystems technology at the University of Freiburg, Germany, and received his Ph.D. from the University of Freiburg/Fraunhofer ISE in 2010. He stayed on as a scientist at Fraunhofer ISE, where he is now head of the group focusing on cleanroom technologies for high-efficiency silicon solar cells.



**Florian Schindler** received his diploma degree in physics in 2011 from the University of Freiburg, Germany, in collaboration with Fraunhofer ISE. In 2015 he was awarded a Ph.D., again in collaboration with Fraunhofer ISE, by the University of Freiburg. The research for his thesis focused on the electrical material properties and efficiency limits of compensated and multicrystalline silicon. He currently holds a postdoc position in the material and cell analysis group at Fraunhofer ISE.



**Stephan Riepe** received his Bachelor's from the University of Sydney, Australia, and his diploma degree in physics from the University of Freiburg, Germany, in 1999 and 2001 respectively. He then joined Fraunhofer ISE, working on silicon characterization. Since receiving his Ph.D. from the University of Konstanz, Germany, in 2008 for his work on efficiency-limiting defects in multicrystalline silicon, he has been head of the crystallization and wafering research group at Fraunhofer ISE.



**Patricia Krenckel** received her Bachelor's and Master's in solid-state and material physics from the University of Göttingen, Germany, in 2010 and 2012 respectively. Currently working on her Ph.D. thesis at Fraunhofer ISE in collaboration with the University of Konstanz, Germany, she is investigating the development of the crystal structure of silicon during ingot casting.



**Armin Richter** received a Ph.D. in physics in 2014 for his work on the development of n-type silicon solar cells and an in-depth characterization of Al<sub>2</sub>O<sub>3</sub>-based silicon surface passivation. His research interests include atomic layer deposition for PV applications, a fundamental understanding of surface passivation, and the development of high-efficiency silicon solar cells along the entire process chain.



**Ralph Müller** received his Masters's in microsystems engineering in 2011 from the University of Freiburg, Germany, in collaboration with Fraunhofer ISE. In 2016 he obtained his Ph.D. from the University of Freiburg, with a thesis topic of ion implantation for high-efficiency silicon solar cells. He is currently a postdoctoral researcher at Fraunhofer ISE.



**Hubert Hauser** studied microsystems engineering at the University of Freiburg, Germany, and received his Ph.D. from the University of Freiburg in 2013. His thesis concerned the development of nanoimprint lithography processes for PV applications. Since his graduation he has been working as a scientist in the micro- and nanostructured surfaces group at Fraunhofer ISE.



**Frank Feldmann** holds a Master's and a Ph.D. in electrical engineering from RWTH Aachen and the Albert Ludwig University of Freiburg respectively. In 2016 he was awarded the Junior Einstein Award, sponsored by SolarWorld AG, for the development of the TOPCon technology, which enables efficiencies beyond 25%. He is currently a postdoctoral researcher at Fraunhofer ISE.



**Bernhard Michl** studied physics at the University of Mainz, Germany, and received his diploma degree in 2008. The research for his diploma thesis on series resistance imaging was carried out at Schott Solar, Alzenau, Germany, in conjunction with Fraunhofer ISE. For his Ph.D., he focused on the characterization of mc-Si material and the efficiency limits in high-efficiency mc-Si solar cells. Up until 2017

he has been working as a postdoc in the material and solar cell characterization group at Fraunhofer ISE.



**Martin C. Schubert** studied physics at the Universities of Montpellier, France, and Freiburg, Germany, and received his Ph.D. in physics in 2008 from the University of Konstanz, Germany. From 2013 to 2014 he was with JAXA and Meiji University, Japan, as a guest professor. He is currently head of the characterization and simulation department at Fraunhofer ISE.



**Dr. Martin Hermle** received his Ph.D. in physics in 2008 from the University of Konstanz, Germany. He joined Fraunhofer ISE in 2002, and since 2008 he has been the head of the high-efficiency silicon solar cell department. His main areas of interest include the development of solar cell technologies for high-efficiency silicon solar cells, and the analysis, characterization and modelling of silicon and tandem solar cells.



**Andreas W. Bett** received his diploma degree in physics and diploma degree in mathematics from the Albert Ludwig University of Freiburg, Germany, in 1988 and 1989 respectively. In 1992 he was awarded a Ph.D. in physics by the University of Konstanz, Germany. He joined Fraunhofer ISE in 1987, and was appointed director of the institute in 2017.



**Stefan W. Glunz** received his Ph.D. from the University of Freiburg, Germany, in 1995. He is the director of the solar cells development and characterization division at Fraunhofer ISE, and a professor of photovoltaic energy conversion at the Albert Ludwig University of Freiburg. His research interests include the design, fabrication and analysis of high-efficiency solar cells.

#### Enquiries

Jan Benick  
Fraunhofer ISE  
Heidenhofstr. 2  
Freiburg 79110  
Germany

Tel. +00497614588-5020  
Email: jan.benick@ise.fraunhofer.de  
Website: www.ise.fraunhofer.de